

Application of JET - like perturbation coils for ELM - mitigation in ITER

A. Nicolai¹, U. Daybelge², M. Z. Tokar¹, C. Yarim²

¹*Institut für Plasmaphysik, Forschungszentrum Jülich GmbH, Euratom Association, Trilateral Euregio Cluster, D-52425 Jülich, Germany*

²*Istanbul Technical University, Faculty of Aeronautics and Astronautics, 80626 Maslak, Istanbul, Turkey*

Abstract

The error field correction coils (EFCC) at JET mounted at a significantly larger distance than e.g. the I-coils in DIII-D were effective in ELM suppression. The potential applicability of EFCC-like coils in ITER is investigated here.

The investigated coils for $n=2$ and $n=3$ are placed at the distance $R_{coil} \approx 11m$ from the ITER axis, have a roughly rectangular shape with a side length of $a_{coil} \approx 18m$, the height $h_{coil} \approx 7m$. The ratio of the radial field to the toroidal field is of the order 10^{-4} . The ITER - like plasma ($I_p=14$ MA, $B_t=5.2$ T) is assumed to be elongated ($\epsilon = 1.8$) and D-shaped ($\delta = 0.3$). Due to the large a_{coil} it can be shown by Fourier analysis that with a moderate current of 80 kA the coils produce a $B_{1,1}$ Fourier component of $\approx 10G$ at the plasma edge. Because of the large distance between the coils and the plasma edge the $B_{4,1}$ component is there roughly one order of magnitude smaller. The thickness of the ergodic layer near the x - point, in the transport barrier, is approximately 25 cm.

Introduction

External magnetic field perturbations have been successfully applied to mitigate type I ELMs [1] which would dramatically increase erosion and cause cyclic heat loads on divertor target plates in a reactor. Therefore coils analogous to the I-coils in DIII-D [1] being mounted relatively close to the plasma have been proposed for ELM mitigation in ITER [2]. However, due to the interference with other device components the application of such coils may be technically difficult. Moreover, recent experiments on JET [3] demonstrate that the error field correction coils (EFCC) mounted at a significantly larger distance from the plasma, are also effective in ELM suppression. In the vacuum approximation the coils produce large Fourier components of low multipolarity which may lead to locking of MHD unstable modes and to disruption. This, however, was not observed in JET-plasmas where toroidal rotation has been induced by unbalanced NBI with a power of roughly 19 MW. In order to study the

possibility for such a screening in the case of EFCCs similar to those planned for ITER [4] the plasma rotation is modelled by applying the revisited neoclassical theory [5].

Magnetic field structure and screening by plasma rotation

Fourier analysis of the radial field performed at the singular surfaces provides the input for the rotation model. The Fourier sine - coefficients of the radial field B_r are given by $B_{mn_s} = \frac{1}{2\pi^2} \int_0^{2\pi} d\theta^* \int_0^{2\pi} d\phi B_r[\theta(\theta^*), \phi] \sin(m\theta^* - n\phi)$. θ^* is the intrinsic angle with the property that a field line becomes straight in the (θ^*, ϕ) - system. Field line tracing is in this paper the main method to demonstrate the destruction of the flux surfaces in the vicinity of the x - point. We assume that the equilibrium magnetic field and the radial perturbing field can be superimposed independently. Thus the obtained total magnetic field vector can be used to track the field lines [5]. To account for plasma rotation, the flux function ψ_s in the singular layer with the width δ_s can be inferred from Ampere's and Faraday's law [5]. Since the eddy currents in a rotating singular surface impede the penetration of the radial field, the 'screened' Fourier component is given by $B_{m,n}^s = B_{m,n}^v \frac{1}{\sqrt{\alpha^2 + (\omega\tau_{VR}f_\tau)^2}}$. $\alpha = \frac{-\Delta'}{2m}$ is of the order unity because the tearing mode index Δ' was estimated in [5] as $-\Delta' \approx 5$. ω is the slip frequency, $\tau_{VR} = 2.104 \frac{r_s}{\delta_s} \left(\frac{\tau_r}{\tau_v}\right)^{\frac{1}{3}} \tau_H^{\frac{2}{3}} \tau_r^{\frac{1}{3}} f_{geo}$ the characteristic time of the singular layer in the 'visco - resistive' regime [6]. τ_r , τ_v , τ_h are the resistive, viscous and the hydrodynamic times of the layer. $f_\tau = \frac{r_s}{2m\delta_s} = \left(\frac{\tau_h}{\tau_v}\right)^{-\frac{1}{6}} \left(\frac{\tau_h}{\tau_r}\right)^{-\frac{1}{6}} \frac{1}{2m}$ is a factor which depends very weakly on the plasma parameters. $f_{geo} = (1 + 2q^2)^{1/3}$ accounts for inertia and δ_s is the thickness of the singular layer.

The main result of the revisited neoclassical theory [5] are the equations describing the radial transport of toroidal and poloidal momentum in a collisional subsonic plasma with steep gradients[5]. They account for parallel, perpendicular and gyro - viscosity, the friction caused by the neutral gas, the momentum source due to neutral beam injection, the braking due to pressure anisotropization evoked by helical perturbation fields, the force density due to the $\vec{j} \times \vec{B}$ force at the singular layer [5], respectively.

Results

The ITER - data are taken from [4]: Major radius $R_0=620$ cm, minor half axis $a=200$ cm, effective radius $r_{max}=270$ cm, plasma current $I_p=14$ MA, toroidal field $B_t=5.2$ T, NBI - power $P_{NBI}=50$ MW, $E_{NBI}=380$ MeV. The maximum toroidal speed is then $v_{t_{max}}=120$ km/sec. The $n=2$ configuration of Fig. 1 yields the spectrum of Fig. 2 which shows that the $m=1, n=2$ component strongly dominates. Since there is no resonance, it does not produce an island but it is important for the ergodization of the separatrix. The $n=1$ - configuration can

be achieved by changing the current direction in two coils of Fig. 1 thus making the current directions in two neighboring coils parallel. Two coil pairs have then the opposite current direction. This configuration yields the spectrum of Fig. 3 which shows that the $m=1, n=1$ component strongly dominates. Since there is no resonance it does not produce an island but it is important for the ergodization of the separatrix. The spectrum for the $n=3$ configuration of Fig. 4 which has the same toroidal mode number as the configuration proposed in [4] is analogous to that in Fig. 2. The dominant components decay now along the line $n=3$. The rotation model yields the toroidal rotation velocity and thus the screening factor S_f (Fig. 5). The rotation profile is for $r_{eff} < 200$ m parabolical and the screening profile has the inflection point (with vanishing curvature) at $r_{eff_i} \approx 180$ cm and a transition length of ≈ 50 cm.

The results of the Fourier analysis (Fig. 3) and of the screening model are consistent with the field line tracing shown in Fig. 6 ($n=1$). At the x - point (of the unperturbed separatrix) the screening is negligible because of the small toroidal velocity. The thickness Δ_m of the ergodized layer is around 25 cm. Since the poloidal extension is restricted to $[230^0 - 300^0]$ the $q=2$ island chain is only partly visible. Due to screening the radial extension is strongly reduced. The remnant $q=3$ islands are visible in a plot with the full poloidal extension but the radial extension is very small.

References

- [1] T.E. Evans, R. A. Moyer, K. H. Burrell et al. Nature Physics, 2 (2006) 419
- [2] M. Becoulet, E. Nardon, G. Huysmans, P. Thomas, Modelling of Edge Control by Ergodic Fields in DIII-D, JET and ITER, 21st IAEA Fusion Energy Conference, Chengdu (2006) paper TH/P1 - 29
- [3] Y. Liang, H. R. Koslowski, P. R. Thomas, E. Nardon et al. submitted to PRL (2006)
- [4] Summary of the ITER Final Design Report, Presented by the ITER Director, Report ITER/G A0 FDR 4 01-07-21 R 0.4, Y. Gribov, private comm., ITER, Cadarache (2007)
- [5] A. Nicolai, U. Daybelge, C. Yarim Nucl. Fus.44 (2004) S93 - S107
- [6] A. Cole, R. Fitzpatrick, Phys. Plasmas 13 (2006) 032503

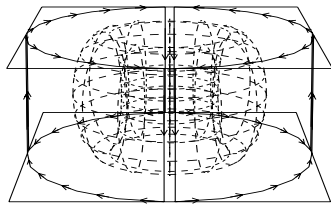


Figure 1: Perturbation coils configured for $n=2$ where two neighboring coils have the opposite current direction

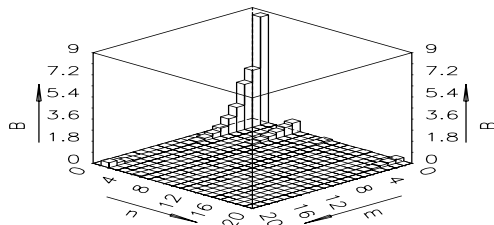


Figure 2: The spectrum for the $n=2$ configuration in Fig. 1. The $(m=1, n=2)$ component is the largest (9G), followed by $(m=2, n=2)$ - component $B_{2,2} \approx \frac{1}{2}B_{1,2}$.

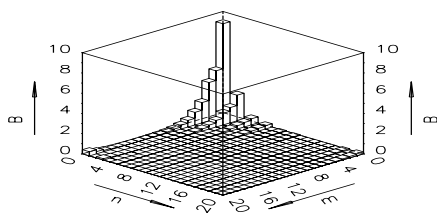


Figure 3: The spectrum for the $n=1$ configuration with parallel currents in neighboring coils of Fig. 1. The shape of the spectrum is similar to that of Fig 2. The $(m=1, n=1)$ component is the largest (10G), followed by $(m=2, n=2)$ - component.

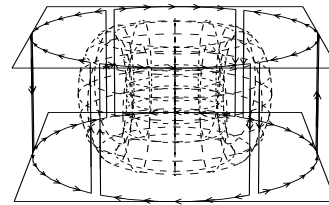


Figure 4: Perturbation coils configured for $n=3$ where two neighboring coils have the opposite current direction

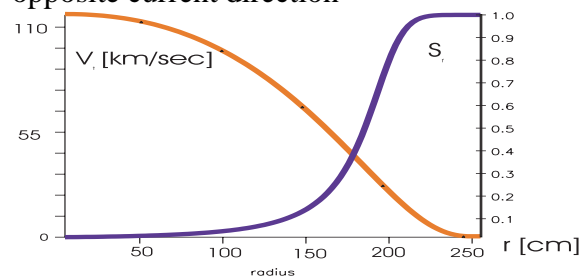


Figure 5: Toroidal velocity profile and screening factor for $P_{NBI} = 50$ MW. The radius of the inflection point of the screening factor is ≈ 180 cm and the transition length is ≈ 50 cm.

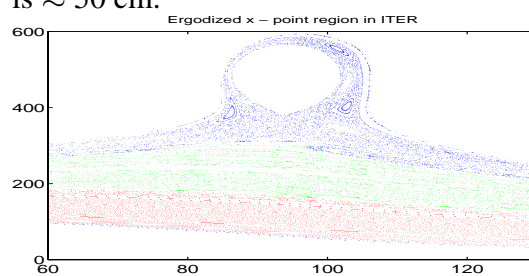


Figure 6: Poincaré - plot for the $n=1$ configuration in Fig. 1 in toroidal coordinates (r, θ) . The ergodized region around the unperturbed x-point ($\Delta_m=25$ cm) clearly visible. The $q=2$ island can be seen only partly because the restricted poloidal extension $[230^0 \dots 300^0]$.